Highlighting the Role of Lubricant Oil in the Development of Hydrogen Internal Combustion Engines by means of a Kinetic Reaction Model

Highlighting the Role of Lubricant Oil in the Development of Hydrogen Internal Combustion Engines by means of a Kinetic Reaction Model

E. Distaso[1*], G. Calò[1], R. Amirante[1], P. De Palma[1], M. Mehl[2], M. Pelucchi[2], A. Stagni[2], P. Tamburrano[1]

[1] Department of Mechanics, Mathematics and Management, Politecnico di Bari, Italy

[2] Department of Chemistry, Materials, and Chemical Engineering, Politecnico di Milano, Italy

* Corresponding author's e-mail: elia.distaso@poliba.it

Abstract. The urgent need to reduce the dependence on fossil fuels has re-ignited the interest toward Hydrogen Internal Combustion Engines (HICEs). Nevertheless, there are still criticalities that need to be assessed for accelerating the development of this technology. The undesired but unavoidable participation of lubricant oil to the combustion process can be the cause of many of these. Due to an extremely low autoignition resistance at low temperatures, lubricant oil is considered the main responsible for the onset of abnormal combustion modes, which need to be understood for delivering reliable and ready to market HICEs. By employing a kinetic reaction mode, this work analyses the autoignition tendency of hydrogen contaminated with n-$C_{16}H_{34}$ (n-hexadecane), the latter being selected as a surrogate species representative of lubricant oil chemical characteristics. Starting from the detailed CRECK model (Version 2003), a reduced mechanism with very small size (169 species and 2796 reactions) was developed, which makes it suitable for the use in practical CFD engine simulations. Zero-dimensional numerical simulations were performed employing the reduced mechanism to quantify the variation of hydrogen ignition delay time due to the presence of different amounts of lubricant oil. Operating conditions typical of engine chambers were considered in the analysis. The results show that lubricant oil can have a significant impact on the charge reactivity, especially in the low-temperature range, with consequences that can potentially hamper the development of HICEs.

1. Introduction

The negative impacts of climate change are mounting very fast and bold actions are required [1]. Greenhouse Gas (GHG) emissions from transport are major contributors to both climate change and air pollution, so that significant efforts are needed to improve the current technologies for mobility. Internal combustion engines need radical modifications to be still considered a sustainable option for the future [2]. It has become imperative to develop innovative combustion techniques [3–6] together with new strategies for controlling the combustion process [7–9] based on the implementation of more accurate and cost-effective sensors [10–12].

However, the most significant contribution to the GHG emissions abatement relies on the exploitation of carbon-neutral and low emission fuels. Hydrogen represents one of the most attractive alternatives to current fossil fuels, offering a strategically sound approach towards a rapid transition to a carbon-free mobility, especially with respect to the land and marine heavy-duty vehicles [13,14]. However, the development of efficient and reliable Hydrogen Internal Combustion Engines (HICEs) still faces some criticalities that prevent such engines from penetrate the marketplace [14–16]. Among these, there is the

spontaneous and premature ignition of the charge, with consequent loss of combustion phasing control that leads to knocking and possibly mechanical engine failure. This problem limits the engine power output by forcing a very lean operation [16–18].

These undesired events were initially ascribed to the presence of richer regions in the chamber. This might be the case for the Direct Injection (DI) mode, for which the achievement of a proper mixing is a really challenging tasks, but it appears unlikely for port fuel injection mode, for which a much better mixing is expected. Presumably, the explanation for the occurrence of premature autoignitions should be sought elsewhere. Hydrogen has a higher auto-ignition temperature compared to petroleum fuels [19], thus its resistance to knocking is expectedly higher. However, its lower ignition energy (one tenth that of gasoline) makes hydrogen easily ignitable by hot spots or residues in combustion chamber. Many recent works have linked the onset of abnormal combustions in HICEs to the presence of "sensitive spots" and lubricating oil, with an extremely low autoignition resistance can play a primary role in their generation [18,20,21].

Lubricant oil can reach the combustion chamber through many different routes [22]: the clearances in the piston-rings system; the positive crankcase ventilation system (i.e., as droplets transported by the blow-by gas stream); the valve stem seals; the turbocharger seals. Moreover, in DI engines, the high-pressure jet will inevitably impact the cylinder walls, entraining oil droplets, and this might be the case not only of liquid fuels but also of gaseous fuel, such as in the case of HICEs [16]. In HICEs, oil contaminations can also originate from the injector lubrication system. Depending on the route, lubricant oil can get into the combustion chamber as liquid, vapor, or as a mist, with different consequences [22,23].

Although it is well-known that lubricant oil can participate to the combustion process, the study of the possible side effects has gained attention only recently due to the need of developing highly boosted DI gasoline engines. Such engines suffer from the occurrence of particularly violent detonation phenomena, especially when operate at low-speed and high-load [24–26]. Several experimental studies showed that the presence of lubricant inside the combustion chamber has a substantial accelerating effect on gasoline ignition [27–30]. In the case of HICEs, the effects can be even more relevant. It has been shown that n-C_7H_{16} can shorten the Ignition Delay Time (IDT) of H_2/air mixtures in the low-temperature range, up to more than one order of magnitude [31], and even trace amounts can significantly modify the ignition behaviour of the charge. The main components of base oils are C15–C54 normal alkanes [32], which are significantly more reactive than n-C_7H_{16}.

It is crucial to study the reaction paths involved in lubricant oil oxidation and to understand how this indispensable element interacts with hydrogen. All past research dedicated to lubricant oil chemical modelling has been focused on gasoline engines [33–38]. However, some general indication about lubricant oil chemical characteristics can be inferred from those studies and directly transferred to the case of HICEs. Studies carried out by different research groups have shown that it is possible to emulate the lubricant oil chemical behaviour by using a single n-alkane molecule as surrogate, namely n-$C_{16}H_{34}$ (n-hexadecane) [35–37]. In a previous study [37], this approach was successfully employed in the development of the so-called "GasLube" reaction mechanism to predict gasoline IDT variations induced by the presence of lubricant oil.

For the sake of completeness, it must be mentioned that lubricant oil can produce additional deleterious effects that still need to be understood. Oil contamination can represent a non-negligible source for soot particles, as pointed out by recent experiments [23,39–42] The formation of lubricant-oil-derived particles in the finest and most dangerous range size (lower than 30 nm) was demonstrated independently from the fuel feeding the engine [23,42]. The long-chained hydrocarbons constituting lubricant oil enhance soot precursor formation [43,44]. Moreover, in-cylinder carbonaceous deposits and floating particles can serve as hot spots able to prematurely ignite the mixture [26], highlighting a possible secondary way by which lubricant oil can promote pre-ignition events.

The aim of this work is to shed light on lubricating oil potential of altering the charge reactivity in HICEs. A reduced kinetic mechanism was developed to this very purpose, selecting n-$C_{16}H_{34}$ as lubricant oil surrogate species. The detailed CRECK model (Version 2003) was used as the reference

kinetic model for deriving a reduced mechanism having a small size, so that it can be also used in practical CFD engine simulations. The mechanism was employed in Zero-Dimensional (0D) simulations with the aim to quantify the effects that lubricant oil can have on hydrogen IDT in engine-like conditions. All the simulations were conducted considering the closed homogeneous batch reactor model with constant volume assumption for solving the time-dependent balance equations for the total mass, the gas-phase species mass, and the energy. A criterion for the IDT evaluation based on the maximum OH and/or CH increase was used.

2. Reduced mechanism development and validation

The detailed CRECK chemical model (Version 2003) [45–47], selected for the development of a reduced mechanism for H_2/n-$C_{16}H_{34}$/air mixtures, is composed of several hierarchically organized and self-consistent sub-models, which have been extensively validated against experimental data collected over a wide range of operating conditions with different facilities (such as flow reactors, shock tube, jet-stirred reactor). More specifically, the detailed mechanism includes a hydrogen sub-mechanism from Kéromnès et al. [48]; a C1-C2 sub-mechanism from Metcalfe et al. [49]; a C3 and molecular growth pathways from Burke et al. [50] and Ranzi et al. [46,51], updated by Bagheri et al. [52]. The detailed kinetic mechanism for high- and low-temperature oxidation consists of 492 species and 17790 reactions.

2.1. Mechanism reduction

The reduction was developed employing the software DoctorSMOKE++, a numerical code based on the open-source software OpenSMOKE++ [53]. More details about the reduction methodology and the software are provided in previous studies [54,55]. For the reduction process the following conditions were considered: temperature values between 500 and 2500 K; pressures values between 1 to 50 bar; equivalence ratio values between 0.5 and 4. The resulting reduced mechanism consists of 169 species and 2796 reactions, with a reduction in the number of species of about 70%.

2.2. Mechanism validation

In order to verify that the reduction process did not affect the accuracy in predicting IDT values, the results of the reduced mechanism were compared with those of the detailed version, which was used as reference. For the comparison, 0D simulations were performed considering a wide range of operating conditions. Namely, the temperature was varied from 500 K to 2000 K the pressure from 5 to 50 bar and the equivalence ratio from 0.5 to 2.0. As an example, Figure 1 reports the results obtained for pure H_2 and n-$C_{16}H_{34}$ for operating conditions that are of interest for the specific purpose of this work. The IDT curves related to the reduced mechanism match those of the detailed mechanism in a very satisfactory way. Similar results were obtained for the remaining operating conditions considered for the validation, which were not reported for the sake of brevity.

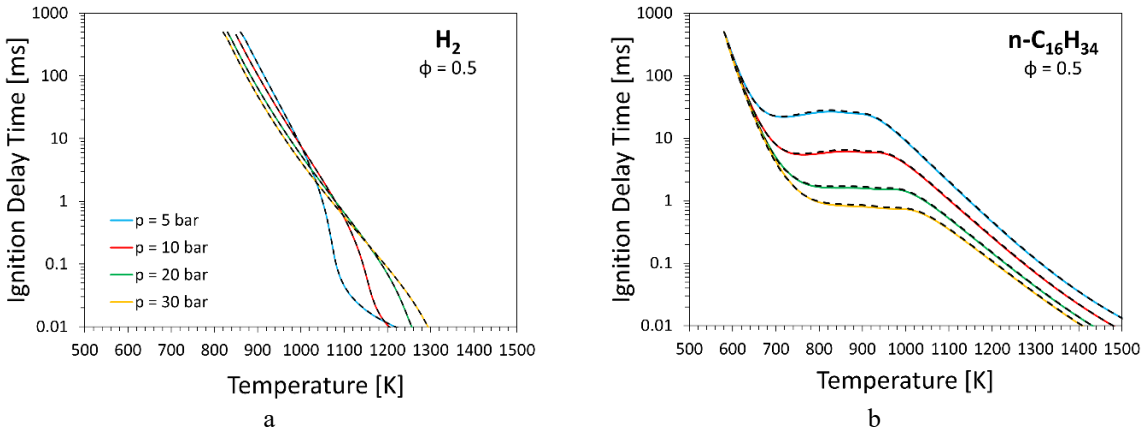

Figure 1. Comparisons between reduced (solid lines) and detailed (dashed lines) mechanisms, in the case of H_2/air (a) and n-$C_{16}H_{34}$/air (b) mixtures at an equivalence ratio (ϕ) equal to 0.5.

3. Analysis of lubricant oil impact on hydrogen reactivity

3.1. Numerical setup

0D numerical simulations employing the developed reduced mechanism were performed in order to highlight the influence of lubricant oil on the H_2 autoignition behaviour. The analysis was performed considering operating conditions consistent with those achievable in an engine cylinder during the compression stroke and in the early stages of combustion. Namely, the temperature was varied in the range 500 - 1300 K, and four different pressures were considered, namely, 5, 10, 20 and 30 bar. An equivalence ratio equal to 0.5 was selected for this analysis, as representative of lean operating conditions. The mixture ignitability was assessed considering a maximum time interval of 500 ms, because longer IDT values are not of interest for engine applications. A comparison between the reactivity characteristics of the two pure species, namely H_2 and n-$C_{16}H_{34}$ was first performed. The effects of the addition of the lubricant oil surrogate species to H_2 were subsequently investigated.

3.2. Results

Figure 2 compares the ignition behaviour in air of n-$C_{16}H_{34}$ with that of H_2, in terms of IDT variations with temperature. It is noticeable that n-$C_{16}H_{34}$ reactivity extends to temperatures significatively lower in comparison to H_2, confirming that lubricant oil can be effectively ignited at temperatures much lower than H_2. In the low-to-intermediate temperature regime, the lubricant oil surrogate remains more reactive than H_2 and only at very high temperatures (> 1000 K) the latter shows shorter IDT values.

The extremely different molecular structure of the two species is at the basis of the quite different behaviour observed in Figure 2. The IDT curves of n-$C_{16}H_{34}$ present the typical shape associated with long-chain hydrocarbon oxidation and due to the existence of the Negative Temperature Coefficient (NTC) regime. Heavy aliphatic hydrocarbons, such as n-$C_{16}H_{34}$, show high reactivity in the low-temperature regime due to the chemistry associated with the so-called “cool flames” (also involved in engine knock phenomena). The linear structure and the large number of secondary $C-H$ bonds in the n-$C_{16}H_{34}$ molecule facilitates the initial H-abstraction step, in which the related alkyl radical is produced. After multiple oxygen-addition and isomerization steps, ketohydroperoxide species are formed and readily decomposed in a degenerate chain branching process that is at the basis of the low-temperature heat release in the cool flame regime. As temperature increases, the IDT of n-$C_{16}H_{34}$ rapidly decreases. However, at intermediate temperatures, the alkyl radical interaction with O_2 is more likely to produce the conjugate alkene together with an HO_2 radical, which does not contribute to chain branching, but rather tends to form the metastable H_2O_2. The olefines generation and the interruption of the chain branching process determine the entrance into the NTC regime, associated with the non-monotonic segment of the n-$C_{16}H_{34}$ IDT curve. As temperature is further increased, the H_2/O_2 system starts to dominate the oxidation process, with the branching reactions involving H_2O_2 decomposition becoming increasingly important. As a consequence, the n-$C_{16}H_{34}$ IDT curve resumes its rapid decrease with temperature.

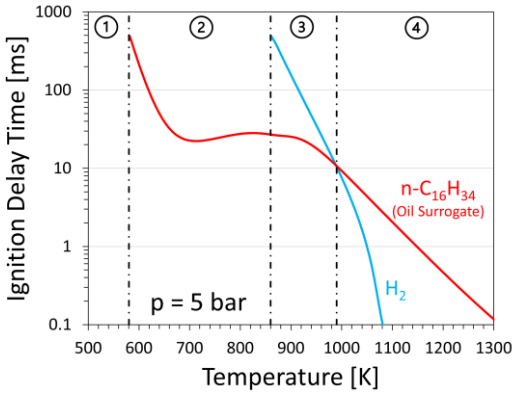

Figure 2. Comparison between the IDT curves of H_2/air and n-$C_{16}H_{34}$/air mixtures, obtained with the reduced mechanism at 5 bar and an equivalence ratio equal to 0.5.

The IDT curves of H_2 show a clear monotonic trend over the entire temperature range depicted in Figure 2. However, in the high-temperature regime it is possible to notice a steeper decrease of the IDT curve (cf. also Figure 1). Such a change of the slope is attributable to the transition from the weakly to the strongly explosive behaviour observed for H_2/air mixtures [56]. It is worth to mention that the pressure range of interest for engine applications is that associated with the third explosion limit of the H_2/O_2 system. In this range, for temperatures slightly above the third limit, the HO_2 chemistry dominates, while for significatively higher temperatures the $H + O_2$ branched-chain mechanism speeds up the H_2 oxidation process. The transition in explosivity is delimited by the extended second explosion limit, and it is visible at around 1050 K in Figure 2.

As a consequence of the quite different behaviour shown by the two species, different conditions can be established according to the initial temperature. In particular, four regions have been identified and they are highlighted in Figure 2. Region 1 is a non-explosive region, in which neither n-$C_{16}H_{34}$/air nor H_2/air mixtures can be ignited due to excessively low temperatures. The upper limit of this region is defined as the lowest n-$C_{16}H_{34}$ ignition temperature at a given pressure. In region 2, n-$C_{16}H_{34}$ shows explosive behaviour, while the temperatures remain still too low for promoting H_2 ignition. The lowest H_2 ignition temperature at a given pressure determines the boundary between region 2 and 3. In region 3, although the temperatures are sufficiently high to ignite H_2, the related IDT values are longer than those of n-$C_{16}H_{34}$, indicating that H_2 remains less reactive than n-$C_{16}H_{34}$ in this region. Region 4 is the high-temperature region, in which H_2 becomes more reactive than n-$C_{16}H_{34}$. The limit that separates region 3 from region 4 is located at a temperature slightly lower than that at which the H_2/O_2 system starts to show a strongly explosive behaviour and dominates the oxidation process.

The existence of region 2 and 3 is a first indication that lubricant oil can represent a potential problem for HICEs. It is remarkable that these regions cover a significatively large temperature range. In region 2, the temperatures are relatively low and, most importantly, comparable with the values obtainable in an engine cylinder during the compression stroke before combustion. These temperatures are well below the H_2 ignition limit, thus not considered potentially dangerous for the regular operation of the engine if the analysis is restricted to the H_2 chemical characteristics. Moreover, in region 3, the IDT values of n-$C_{16}H_{34}$ are significatively lower than those of H_2. Although the temperature starts to be relatively high in this region, there might still be some chances to generate undesired charge autoignition around the Top Dead Centre (TDC) or even later (e.g., in the end-gas, in the case of spark-ignition engines).

Figure 3 shows the effects that a pressure increase produces on the IDT curves and thus on the relative extension of the four regions. The pressure has a drastic influence on n-$C_{16}H_{34}$ reactivity, so that an its increase makes the related IDT curve moving down to significantly lower times. In addition, the NTC region is shifted towards higher temperatures, and it becomes progressively less pronounced with the pressure increase (starting from 20 bar the curve is monotonic). It is worth noting that at 20 bar (Figure 3-c), n-$C_{16}H_{34}$ shows an IDT value at 700 K equal to that shown by H_2 at about 1000 K (i.e., 5 ms). At 30 bar (Figure 3-d) a temperature of 780 K is sufficient to ignite a n-$C_{16}H_{34}$/air mixture in about 1 ms, while it is necessary to reach about 1070 K in order to achieve the same result with a H_2/air mixture.

The lower limit of region 2 seems to be not very sensitive to pressure variations, remaining stable around 580 K. The upper limit of region 2 is slightly lowered by the pressure increase, and it moves from about 860 K at 5 bar (Figure 3-a) to about 820 K at 30 bar (Figure 3-d). Consequently, the temperature range defining the extension of region 2 tends to be slightly narrowed by the pressure increase. This, in combination with the modifications that the n-$C_{16}H_{34}$ IDT curve undergoes with the pressure increase, determines that region 2 includes both the cool flame and NTC regimes at lower pressures (cf. Figure 3-a and -b), while it becomes almost entirely occupied by the cool flame regime at higher pressures (cf. Figure 3-c and -d). During the last part of the compression stroke, the in-cylinder pressure can reach values comparable to those related to Figure 3-c and -d. Therefore, if thermodynamic conditions suitable for a premature ignition of the charge are established, such a pre-ignition event is surely the consequence of the low-temperature heat release involved in the cool flame chemistry that characterizes the long-chained hydrocarbon species composing lubricant oil.

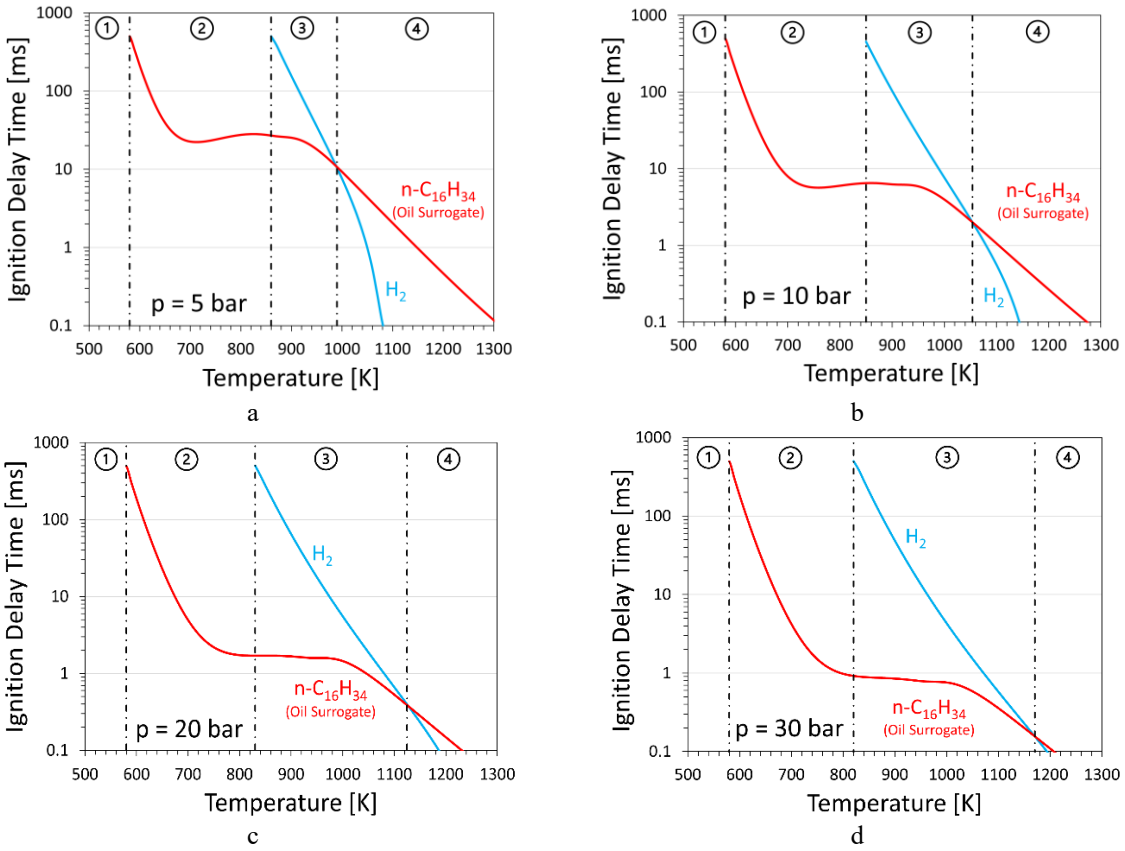

Figure 3. Effects of pressure variations on the IDT curves of H_2/air and n-$C_{16}H_{34}$/air mixtures, obtained with the reduced mechanism at an equivalence ratio equal to 0.5.

At high pressures (Figure 3-c and -d), the n-$C_{16}H_{34}$ IDT value remains almost constant for a large portion of region 3. Near the lower limit of region 3, the difference between the IDT values of n-$C_{16}H_{34}$ and H_2 is larger than two orders of magnitude, which suggests that at least the first half of this region needs to be taken under consideration. The limit that separates region 3 from region 4 (namely, the reactivity crossing point) moves to higher temperatures with the pressure increase. As a result, the temperature range in which n-$C_{16}H_{34}$ remains more reactive than H_2 is extended by the pressure increase. This is linked to the shifting of the transition from weakly to strongly explosive behaviour of the H_2/O_2 system to higher temperatures with the pressure increase, as it is possible to infer from both Figure 3 and Figure 1, and in accordance with what has been previously observed [56,57].

The results shown in Figure 3 highlight the difference in reactivity that exists between the two pure species at the same stoichiometry (i.e., for an equivalence ratio equal to 0.5). However, it must be observed that the two species require a significatively different amount of air for obtaining the same equivalence ratio value, and this is due to the great difference existing between the two molecular structures. In the engine combustion chamber, the amount of air is that required for oxidizing the fuel at a given operating condition. When oil droplets are released, a gaseous mixture of oil and fuel can form and react with the available air. As a result, a local increase of the fuel-to-air ratio can be observed where oil is entrained in the charge. Trace amounts of n-$C_{16}H_{34}$ in H_2 suffice to significantly change the local stoichiometry. Considering a H_2/air mixture having an initial equivalence ratio, ϕ_{H_2}, equal to 0.5, Figure 4 shows that a volume fraction of n-$C_{16}H_{34}$ in the n-$C_{16}H_{34}$ /H_2 mixture, χ_{oil}, equal to 0.01 produces a total equivalence ratio, ϕ_{tot}, equal to 0.75. Locally stoichiometric conditions (i.e., ϕ_{tot} = 1) are reached with χ_{oil} = 0.02. For χ_{oil} = 0.1, the total equivalence ratio reaches a value of 3.2.

This consideration points out that lubricant oil can increase the local reactivity of the charge for two reasons: the first is due to its own molecular structure, which makes it highly reactive (significantly

more than H_2) in the low-temperature regime; and the second it is because its addition to the fuel/air mixture produces a non-negligible local enrichment of the charge. The two combined effects were investigated by performing simulations in which the volume fractions of n-$C_{16}H_{34}$ in H_2, namely χ_{oil}, was varied from 0 to 0.1 and with the total equivalence ratio, ϕ_{tot}, varied accordingly to the trend reported in Figure 4. The initial H_2/air mixture equivalence ratio in absence of n-$C_{16}H_{34}$ was considered equal to 0.5 (i.e., for χ_{oil} = 0, $\phi_{tot} = \phi_{H_2}$ = 0.5). With this approach it was possible to analyse thermochemical conditions resembling those that can be locally generated in the combustion chamber of an engine where lubricant oil contamination occurs.

Figure 5 reports the IDT curves of the considered H_2/n-$C_{16}H_{34}$/air mixtures at the same pressures considered in the previous analysis related to the pure species. The IDT curves relative to n-$C_{16}H_{34}$/air mixtures at an equivalence ratio equal to 0.5 are also reported as reference (dashed red lines). Figure 5 points out that an oil volume fraction, χ_{oil}, comprised between 0.03 and 0.04 is sufficient to obtain an IDT curve close to that of pure n-$C_{16}H_{34}$. For χ_{oil} between 0.01 and 0.03, the IDT curves are comprised between those of pure n-$C_{16}H_{34}$ and H_2. For χ_{oil} larger than 0.04, the H_2/n-$C_{16}H_{34}$/air mixtures show reactivity even higher than that of pure n-$C_{16}H_{34}$ due to the increased fuel-to-air ratio. As a result, the part of the IDT curve associated with the NTC regime is shifted down towards increasingly shorter IDT values as χ_{oil} is progressively increased.

It must be observed that the comparison between mixture reactivities is not sufficient alone to determine whether the conditions reigning in the combustion chamber can promote premature autoignition. A comparison of the IDT values with the typical residence times of the charge is also needed. For instance, in an engine running at 1000 rpm, the piston needs roughly 30 ms to travel from the bottom dead centre to the TDC; thus 15 ms are needed to complete the latter half of the compression stroke. This time decreases to 3 ms at 5000 rpm. Heavier engines probably run at lower speeds and more time is required. As a reference, one can consider that, for an engine speed equal to 150 rpm, the time to cover one half of the stroke is about 100 ms. These time intervals are comparable with the IDT values that H_2/n-$C_{16}H_{34}$/air mixtures show in region 2 and 3 (cf. Figure 5).

At 5 bar (Figure 5-a), for χ_{oil} between 0.05 and 0.1, it is possible to obtain an IDT value lower than 10 ms in region 2 starting from a temperature higher than 700 and 680 K, respectively. However, these temperatures are seldom reached at the beginning of the compression, namely when this relative low-pressure level can be reached.

At 10 bar (Figure 5-b), IDT values comprised between 10 and 100 ms can be obtained with a temperature between 630 and 700 K already with χ_{oil} between 0.02 and 0.03. These thermodynamic conditions can be reached at the half of the compression stroke in an engine having a Compression Ratio (CR) between 10 and 14 and might result critical for engines working at low speed. As an example, if 680 K and 10 bar are reached at 90 CADs before TDC in an engine running at 1000 rpm, then the time needed to reach the TDC (i.e., 15 ms) equates the IDT value of a H_2/n-$C_{16}H_{34}$/air mixtures having χ_{oil} = 0.03. Considering that the piston continues compressing the charge, there might be a high probability of autoignition. Temperatures higher than 680 K are needed to have an IDT shorter than 10 ms, but it is unlikely to obtain that at this pressure (it might be justified by the presence of hot spots).

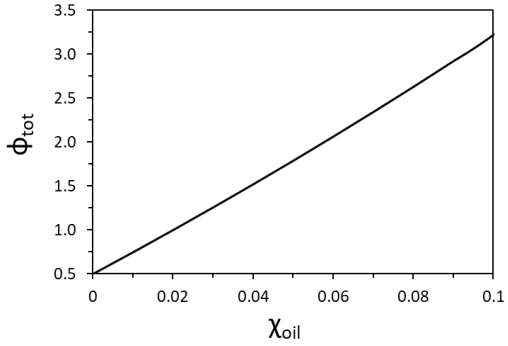

Figure 4. Total equivalence ratio (ϕ_{tot}) variation with lubricant oil surrogate volume fraction (χ_{oil}). The amount of air in the H_2/n-$C_{16}H_{34}$/air mixture is the same of a H_2/air mixture having an equivalence ratio equal to 0.5.

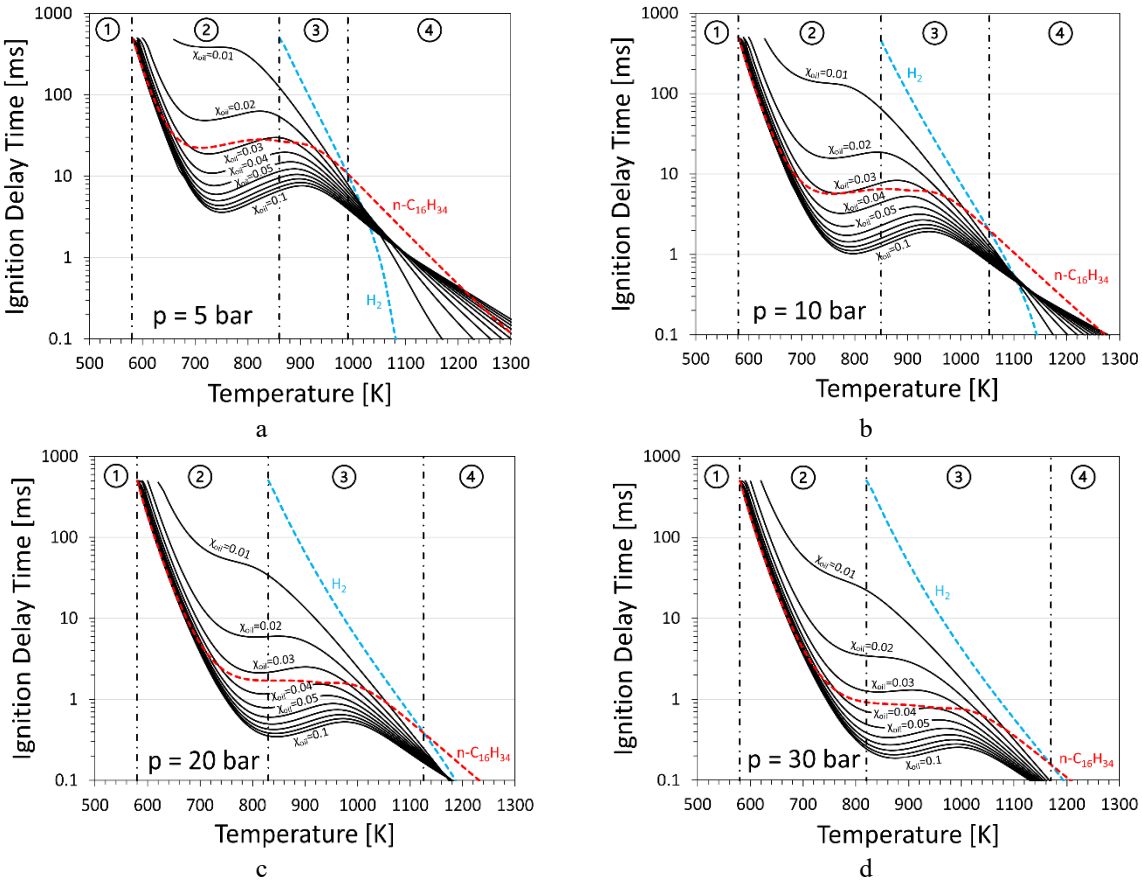

Figure 5. Effects of lubricant oil surrogate (n-$C_{16}H_{34}$) addition on H_2 IDT at different pressures. Light blue dashed lines and red dashed lines refer to H_2/air mixtures and n-$C_{16}H_{34}$/air mixtures at an equivalence ratio equal to 0.5, respectively.

Starting from 10 bar, for χ_{oil} larger than 0.05, the temperature at which the IDT curves go below 10 ms remains approximately constant at about 670 K. At 20 bar (Figure 5-c), the IDT values start to be lower than 1 ms in region 2 for χ_{oil} equal to 0.05 and temperatures higher than 750 K. At 30 bar (Figure 5-d), the same result is obtained at the same temperature but already with a χ_{oil} equal to 0.04.
Figure 5-c and -d show that, at pressures between 20 and 30 bar, a χ_{oil} larger than 0.05 produces IDT values between 1 and 10 ms for temperatures comprised between 680 and 780 K. Such thermodynamic conditions can be reached a few CADs before TDC even for engine with a CR around 12. The higher the CR is the earlier such conditions are reached. With a CR equal to 16, it might be possible to have a pressure of about 20 bar and a temperature of about 800 K around the half of the compression stroke. A mixture with a χ_{oil} between 0.04 and 0.05 would require about 1 ms to ignite in such conditions. The engine should run at about 15000 rpm in order to reach the TDC before autoignition occurs.
For temperatures higher than 780 K, the IDT values results lower than 1 ms starting from a χ_{oil} equal to 0.05 (Figure 5-c and d). With larger values of χ_{oil}, the IDT becomes shorter than 1 ms starting from temperature of 750 K and pressure of 20 bar.

4. Conclusions

The present work represents the first attempt to characterize the effects caused by the interaction of hydrogen with lubricant oil in the combustion chamber of Hydrogen Internal Combustion Engines (HICEs). The analysis aims at ascertaining whether lubricant oil can vary the charge reactivity in a significant way so that it can promote its premature ignition. For this purpose, a reduced reaction mechanism was developed from the detailed CRECK kinetic model (Version 2003), selecting n-$C_{16}H_{34}$

(n-hexadecane) as lubricant oil surrogate species. The mechanism was employed in numerical simulations in order to quantify the variations that lubricant oil can induce in hydrogen Ignition Delay Time (IDT) in engine-like conditions.

The results confirm that lubricant oil can significantly alter the charge reactivity, especially in the low-temperature range. The lubricant oil surrogate species (n-$C_{16}H_{34}$) remains highly more reactive than H_2 for a wide range of temperatures. This result points out that the presence of lubricant oil can facilitate the mixture ignition at temperatures considerably lower than the H_2 autoignition point at a given pressure. Temperatures considered safe for pure H_2 might be potentially dangerous in the case of lubricant oil contamination.

It has been also highlighted that lubricant oil can increase the local reactivity of the charge not only because of its chemical properties, but also because its addition produces a substantial local enrichment effect. For thermodynamic conditions consistent with those achievable in an engine combustion chamber, H_2/n-$C_{16}H_{34}$/air mixtures show IDT values that are comparable to the residence time of the in-cylinder charge during the compression stroke.

The results shown in this work point out that trace amounts of lubricant oil can effectively promote the onset of premature ignitions of the charge in HICEs. The low-temperature heat release associated with the oxidation of the long-chained hydrocarbons composing lubricant oil is at the basis of these potential uncontrolled ignition events. Therefore, the accurate chemical modelling of the fuel-lubricant interaction represents an essential aspect for enabling the further development of the internal combustion engine. Due to the small size, the reduced reaction model presented in this work can be directly used in CFD simulations as an auxiliary tool for providing information difficult or impossible to obtain solely through experiments.

References

[1] Lenton T M, Rockström J, Gaffney O, Rahmstorf S, Richardson K, Steffen W and Schellnhuber H J 2019 Climate tipping points—too risky to bet against *Nature* **575** 592–5

[2] Eckerle W, Sujan V and Salemme G 2017 Future Challenges for engine manufacturers in view of future emissions legislation *SAE Tech. Pap. 2017-01-1923*

[3] Robertson D and Prucka R 2019 A Review of Spark-Assisted Compression Ignition (SACI) Research in the Context of Realizing Production Control Strategies *SAE Tech. Pap. 2019-24-0027*

[4] Distaso E, Amirante R, Cassone E, De Palma P, Sementa P, Tamburrano P and Veglieco B 2020 Analysis of the Combustion Process in a Lean-Burning Turbulent Jet Ignition Engine Fueled with Methane *Energy Convers. Manag.* **223** 113257

[5] Distaso E, Amirante R, Cassone E, Catapano F, De Palma P, Sementa P and Tamburrano P 2019 Experimental and Numerical Analysis of a Pre-Chamber Turbulent Jet Ignition Combustion System *SAE Tech. Pap. 2019-24-0018*

[6] Paykani A, Kakaee A-H, Rahnama P and Reitz R D 2016 Progress and recent trends in reactivity-controlled compression ignition engines *Int. J. Engine Res.* **17** 481–524

[7] Di Mauro A, Chen H and Sick V 2019 Neural network prediction of cycle-to-cycle power variability in a spark-ignited internal combustion engine *Proc. Combust. Inst.* **37** 4937–44

[8] Ravaglioli V, Ponti F, De Cesare M, Stola F, Carra F and Corti E 2017 Combustion Indexes for Innovative Combustion Control *SAE Int. J. Engines* **10** 2371–81

[9] Kuronita T, Sakai T, Queck D, Puts R, Visser S, Herrmann O and Nishijima Y 2020 A Study of Dynamic Combustion Control for High Efficiency Diesel Engine *SAE Tech. Pap. 2020-01-0297*

[10] Amirante R, Casavola C, Distaso E and Tamburrano P 2015 Towards the Development of the In-Cylinder Pressure Measurement Based on the Strain Gauge Technique for Internal Combustion Engines *SAE Tech. Pap. 2015-24-2419*

[11] Ashok B, Ashok S D and Kumar C R 2016 A review on control system architecture of a SI engine management system *Annu. Rev. Control* **41** 94–118

[12] Amirante R, Coratella C, Distaso E, Rossini G and Tamburrano P 2017 Optical device for measuring the injectors opening in common rail systems *Int. J. Automot. Technol.* **18** 729–42

[13] Shinde B J and Karunamurthy K 2022 Recent progress in hydrogen fuelled internal combustion engine (H2ICE) - A comprehensive outlook *Mater. Today Proc.* **51** 1568–79

[14] Faizal M, Chuah L S, Lee C, Hameed A, Lee J, Shankar M and others 2019 Review of hydrogen fuel for

internal combustion engines *J. Mech. Eng. Res. Dev.* **42** 35–46
[15] Hosseini S E and Butler B 2020 An overview of development and challenges in hydrogen powered vehicles *Int. J. Green Energy* **17** 13–37
[16] Yip H L, Srna A, Yuen A C Y, Kook S, Taylor R A, Yeoh G H, Medwell P R and Chan Q N 2019 A review of hydrogen direct injection for internal combustion engines: Towards carbon-free combustion *Appl. Sci.* **9** 1–30
[17] Li Y, Gao W, Zhang P, Fu Z and Cao X 2021 Influence of the equivalence ratio on the knock and performance of a hydrogen direct injection internal combustion engine under different compression ratios *Int. J. Hydrogen Energy* **46** 11982–93
[18] Xu H, Ni X, Su X, Xiao B, Luo Y, Zhang F, Weng C and Yao C 2021 Experimental and numerical investigation on effects of pre-ignition positions on knock intensity of hydrogen fuel *Int. J. Hydrogen Energy* **46** 26631–45
[19] Aleiferis P G and Rosati M F 2012 Controlled autoignition of hydrogen in a direct-injection optical engine *Comb. Flame* **159** 2500–15
[20] Gao J, Wang X, Song P, Tian G and Ma C 2022 Review of the backfire occurrences and control strategies for port hydrogen injection internal combustion engines *Fuel* **307** 121553
[21] Rouleau L, Duffour F, Walter B, Kumar R and Nowak L 2021 Experimental and Numerical Investigation on Hydrogen Internal Combustion Engine *SAE Tech.Papers*
[22] Yilmaz E, Tian T, Wong V W and Heywood J B 2004 The contribution of different oil consumption sources to total oil consumption in a spark ignition engine *SAE TechPapers*
[23] Amirante R, Distaso E, Napolitano M, Tamburrano P, Iorio S D, Sementa P, Vaglieco B M and Reitz R D 2017 Effects of lubricant oil on particulate emissions from port-fuel and direct-injection spark-ignition engines *Int. J. Engine Res.* **18** 606–20
[24] Dahnz C, Han K-M, Spicher U, Magar M, Schießl R and Maas U 2010 Investigations on pre-ignition in highly supercharged SI engines *SAE Int. J. Engines* **3** 214–24
[25] Zaccardi J-M and Escudié D 2015 Overview of the main mechanisms triggering low-speed pre-ignition in spark-ignition engines *Int. J. Engine Res.* **16** 152–65
[26] Wang Z, Liu H and Reitz R D 2017 Knocking combustion in spark-ignition engines *Prog. Energy Combust. Sci.* **61** 78–112
[27] Distaso E, Amirante R, Calò G, De Palma P, Tamburrano P and Reitz R D 2018 Investigation of Lubricant Oil influence on Ignition of Gasoline-like Fuels by a Detailed Reaction Mechanism *Energy Proc.* **148** 663–70
[28] Amann M and Alger T 2012 Lubricant reactivity effects on gasoline spark ignition engine knock *SAE Int. J. Fuels Lubr.* **5** 760–71
[29] Kassai M, Torii K, Shiraishi T, Noda T, Goh T K, Wilbrand K, Wakefield S, Healy A, Doyle D, Cracknell R and others 2016 *Research on the effect of lubricant oil and fuel properties on LSPI occurrence in boosted SI engines*
[30] Kubach H, Weidenlener A, Pfeil J, Koch T, Kittel H, Roisman I V and Tropea C 2018 Investigations on the Influence of Fuel Oil Film Interaction on Pre-ignition Events in Highly Boosted DI Gasoline Engines *SAE Tech. Pap. 2018-01-1454*
[31] Aggarwal S K, Awomolo O and Akber K 2011 Ignition characteristics of heptane-hydrogen and heptane-methane fuel blends at elevated pressures *Int. J. Hydrogen Energy* **36** 15392–402
[32] Wang F C-Y and Zhang L 2007 Chemical composition of group II lubricant oil studied by high-resolution gas chromatography and comprehensive two-dimensional gas chromatography *Energy&Fuels* **21** 3477–83
[33] Huang Y, Li Y, Zhang W, Meng F and Guo Z 2018 3D simulation study on the influence of lubricant oil droplets on pre-ignition in turbocharged DISI engines *Proc. Inst. Mech. Eng. Part D J. Automob. Eng.* **232** 1677–93
[34] Ohtomo M, Suzuoki T, Miyagawa H, Koike M, Yokoo N and Nakata K 2019 Fundamental analysis on auto-ignition condition of a lubricant oil droplet for understanding a mechanism of low-speed pre-ignition in highly charged spark-ignition engines *Int. J. Engine Res.* **20** 292–303
[35] Distaso E, Amirante R, Calò G, De Palma P and Tamburrano P 2021 Lubricant-Oil-Induced Pre-ignition Phenomena in Modern Gasoline Engines: Using Experimental Data and Numerical Chemistry to Develop a Practical Correlation *SAE Tech. Pap. 2021-24-0052*
[36] Gupta A, Shao H, Remias J, Roos J, Wang Y, Long Y, Wang Z and Shuai S-J 2016 *Relative Impact of Chemical and Physical Properties of the Oil-Fuel Droplet on Pre-Ignition and Super-Knock in*

Turbocharged Gasoline Engines
[37] Distaso E, Amirante R, Calò G, De Palma P, Tamburrano P and Reitz R D 2020 Predicting Lubricant Oil Induced Pre-Ignition Phenomena in Modern Gasoline Engines: the Reduced GasLube Reaction Mechanism *Fuel* **281** 118709
[38] Palaveev S, Magar M, Kubach H, Schiessl R, Spicher U and Maas U 2013 Premature flame initiation in a Turbocharged DISI engine - Numerical and experimental investigations *SAE Int. J. Engines* **6** 54–66
[39] Distaso E, Amirante R, Calò G, De Palma P and Tamburrano P 2020 Evolution of Soot Particle Number, Mass and Size Distribution along the Exhaust Line of a Heavy-Duty Engine Fueled with Compressed Natural Gas *Energies* **13** 3993
[40] Distaso E, Amirante R, Tamburrano P and Reitz R D 2018 Steady-state Characterization of Particle Number Emissions from a Heavy-Duty Euro VI Engine Fueled with Compressed Natural Gas *Energy Proc.* **148** 671–8
[41] Amirante R, Distaso E, Tamburrano P and Reitz R D 2015 Measured and Predicted Soot Particle Emissions from Natural Gas Engines *SAE Tech Pap 2015-24-2518*
[42] Amirante R, Distaso E, Di Iorio S, Pettinicchio D, Sementa P, Tamburrano P and Vaglieco B M 2017 Experimental Investigations on the Sources of Particulate Emission within a Natural Gas Spark-Ignition Engine *SAE Tech Pap 2017-24-0141*
[43] Amirante R, Distaso E, Di Iorio S, Sementa P, Tamburrano P, Vaglieco B M and Reitz R D 2017 Effects of natural gas composition on performance and regulated, greenhouse gas and particulate emissions in spark-ignition engines *Energy Convers. Manag.* **143** 338–47
[44] Distaso E, Amirante R, Tamburrano P and Reitz R D 2019 Understanding the role of soot oxidation in gasoline combustion: A numerical study on the effects of oxygen enrichment on particulate mass and number emissions in a spark-ignition engine *Energy Convers. Manag.* **184** 24–39
[45] Ranzi E, Cavallotti C, Cuoci A, Frassoldati A, Pelucchi M and Faravelli T 2015 New reaction classes in the kinetic modeling of low temperature oxidation of n-alkanes *Comb. Flame* **162** 1679–91
[46] Ranzi E, Frassoldati A, Stagni A, Pelucchi M, Cuoci A and Faravelli T 2014 Reduced kinetic schemes of complex reaction systems: fossil and biomass-derived transportation fuels *Int. J. Chem. Kinet.* **46** 512–42
[47] Ranzi E, Frassoldati A, Granata S and Faravelli T 2005 Wide-range kinetic modeling study of the pyrolysis, partial oxidation, and combustion of heavy n-alkanes *Ind. \& Eng. Chem. Res.* **44** 5170–83
[48] Kéromnès A, Metcalfe W K, Heufer K A, Donohoe N, Das A K, Sung C-J, Herzler J, Naumann C, Griebel P, Mathieu O and others 2013 An experimental and detailed chemical kinetic modeling study of hydrogen and syngas mixture oxidation at elevated pressures *Comb. Flame* **160** 995–1011
[49] Metcalfe W K, Burke S M, Ahmed S S and Curran H J 2013 A hierarchical and comparative kinetic modeling study of C1- C2 hydrocarbon and oxygenated fuels *Int. J. Chem. Kinet.* **45** 638–75
[50] Burke S M, Burke U, Mc Donagh R, Mathieu O, Osorio I, Keesee C, Morones A, Petersen E L, Wang W, DeVerter T A and others 2015 An experimental and modeling study of propene oxidation. Part 2: Ignition delay time and flame speed measurements *Comb. Flame* **162** 296–314
[51] Ranzi E, Frassoldati A, Grana R, Cuoci A, Faravelli T, Kelley A P and Law C K 2012 Hierarchical and comparative kinetic modeling of laminar flame speeds of hydrocarbon and oxygenated fuels *Prog. Energy Combust. Sci.* **38** 468–501
[52] Bagheri G, Ranzi E, Pelucchi M, Parente A, Frassoldati A and Faravelli T 2020 Comprehensive kinetic study of combustion technologies for low environmental impact: MILD and OXY-fuel combustion of methane *Comb. Flame* **212** 142–55
[53] Cuoci A, Frassoldati A, Faravelli T and Ranzi E 2015 OpenSMOKE++: An object-oriented framework for the numerical modeling of reactive systems with detailed kinetic mechanisms *Comput. Phys. Commun.* **192** 237–64
[54] Stagni A, Cuoci A, Frassoldati A, Faravelli T and Ranzi E 2014 Lumping and reduction of detailed kinetic schemes: an effective coupling *Ind. \& Eng. Chem. Res.* **53** 9004–16
[55] Stagni A, Frassoldati A, Cuoci A, Faravelli T and Ranzi E 2016 Skeletal mechanism reduction through species-targeted sensitivity analysis *Comb. Flame* **163** 382–93
[56] Wang X and Law C K 2013 An analysis of the explosion limits of hydrogen-oxygen mixtures *J. Chem. Phys.* **138**
[57] Lee D and Hochgreb S 1998 Hydrogen autoignition at pressures above the second explosion limit (0.6-4.0 MPa) *Int. J. Chem. Kinet.* **30** 385–406